



HAL
open science

Exacerbation of the mild steel corrosion process by direct electron transfer between [Fe-Fe]-hydrogenase and material surface

Ingrid Rouvre, Régine Basséguy

► **To cite this version:**

Ingrid Rouvre, Régine Basséguy. Exacerbation of the mild steel corrosion process by direct electron transfer between [Fe-Fe]-hydrogenase and material surface. *Corrosion Science*, 2016, 111, pp.199-211. 10.1016/j.corsci.2016.05.005 . hal-01907316

HAL Id: hal-01907316

<https://hal.science/hal-01907316>

Submitted on 29 Oct 2018

HAL is a multi-disciplinary open access archive for the deposit and dissemination of scientific research documents, whether they are published or not. The documents may come from teaching and research institutions in France or abroad, or from public or private research centers.

L'archive ouverte pluridisciplinaire **HAL**, est destinée au dépôt et à la diffusion de documents scientifiques de niveau recherche, publiés ou non, émanant des établissements d'enseignement et de recherche français ou étrangers, des laboratoires publics ou privés.



Open Archive Toulouse Archive Ouverte (OATAO)

OATAO is an open access repository that collects the work of some Toulouse researchers and makes it freely available over the web where possible.

This is an author's version published in: <http://oatao.univ-toulouse.fr/20507>

Official URL: <https://doi.org/10.1016/j.corsci.2016.05.005>

To cite this version:

Rouvre, Ingrid and Basséguy, Régine Exacerbation of the mild steel corrosion process by direct electron transfer between [Fe-Fe]-hydrogenase and material surface. (2016) Corrosion Science, 111. 199-211. ISSN 0010-938X

Any correspondence concerning this service should be sent to the repository administrator:
tech-oatao@listes-diff.inp-toulouse.fr

Exacerbation of the mild steel corrosion process by direct electron transfer between [Fe-Fe]-hydrogenase and material surface

Ingrid Rouvre, Régine Basseguy*

Laboratoire de Génie Chimique, Université de Toulouse, CNRS, INPT, UPS, Toulouse, France

A B S T R A C T

The influence of [Fe-Fe]-hydrogenase from *Clostridium acetobutylicum* on the anaerobic corrosion of mild steel was studied and the use of a dialysis bag to contain the enzyme in the close vicinity of the electrode surface led to conclusive tests. Electrochemical measurements (open-circuit potential monitoring, corrosion rate evolution, impedance), and surface and medium analysis, all confirmed the strong effect of hydrogenase to exacerbate the corrosion process. Electrolysis performed at a cathodic potential proved that hydrogenase catalysed the electrochemical reduction of protons or water into dihydrogen by direct electron transfer, demonstrating the involvement of hydrogenase in cathodic depolarisation.

Keywords:
Mild steel
Microbiological corrosion
EIS
SEM

1. Introduction

Hydrogenases are produced by microorganisms from diverse phylogenetic classifications, such as dissimilatory metal reducing bacteria [1], fermentative bacteria [2] and methanogenic archaea [3], among others [4]. Hydrogenases, which are either present in bacteria or free in solution, have been identified as key proteins in microbially induced corrosion (MIC) phenomena [3,5–10] but this is still a controversial issue. Even though these enzymes are present in most of the microorganisms involved in corrosion, the participation of hydrogenases in a direct electron transfer mechanism has rarely been demonstrated. Otherwise, free enzymes are often assumed to be unstable but Chatelus et al. [11] have demonstrated that hydrogenases can be stable over months and that their activity does not depend on the presence of viable cells. Thus, bacteria (which contain hydrogenases) or free hydrogenases that are still attached to metallic surfaces may retain their catalysing capabilities for a long time. Yates et al. [12] have also shown that the hydrogen reaction can be enhanced not only by living cells but also by cell debris (including killed microorganisms and hydrogenase).

Hydrogenases are defined as oxidoreductases that have their redox potential at the same potential as the H_2/H^+ redox couple (-410 mV vs standard hydrogen electrode) at ambient standard conditions (25°C , atmospheric pressure, all concentrations 1 M

except for the pH of 7) [12]. In anaerobic conditions, hydrogenases catalyse the reversible reaction shown in Eq. (1) [13–17].



This reduction reaction, which is the driving force of anaerobic corrosion, is generally considered as the rate-limiting reaction in the corrosion process of steel. Two mechanisms of hydrogenase action on corrosion have been established [5,6,18]. The first involves a synergetic effect between hydrogenase and phosphates (or weak acids) in presence of a redox mediator [18–20]. The second mechanism proposed does not require a redox mediator and hydrogenase catalyses the reduction of protons or water by direct electronic transfer [5,6]. The ability of various purified redox enzymes to accept electrons directly from cathodic surfaces has been repeatedly demonstrated [3,7,21,22], and the particular involvement of free hydrogenase in metal corrosion has sometimes been proposed [3,5,6,11]. However, there is no clear demonstration, at this time, of corrosion process catalysis by direct electron transfer between the hydrogenase and the mild steel, that can be considered as a cathodic depolarisation. When investigating the impact of an electromethanogenic archaeon called *Methanococcus maripaludis* (*M.m.*) on the corrosion of iron granules, Deutzmann et al. discovered an apparently direct electron uptake explained by redox-active enzymes, such as hydrogenases [3]. This was demonstrated by using the wild-type strain of *M.m.* and a mutant strain with no hydrogenases. When $\text{Fe}(0)$ -containing vials were amended with the mutant cell-free culture medium, the H_2 formation rate was equivalent to the abiotic control ($51 \pm 7.8\text{ nmol}$ electron equivalents (eeq)/h) whereas, with the wild type

* Corresponding author.
E-mail address: regine.basseguy@ensiacet.fr (R. Basseguy).

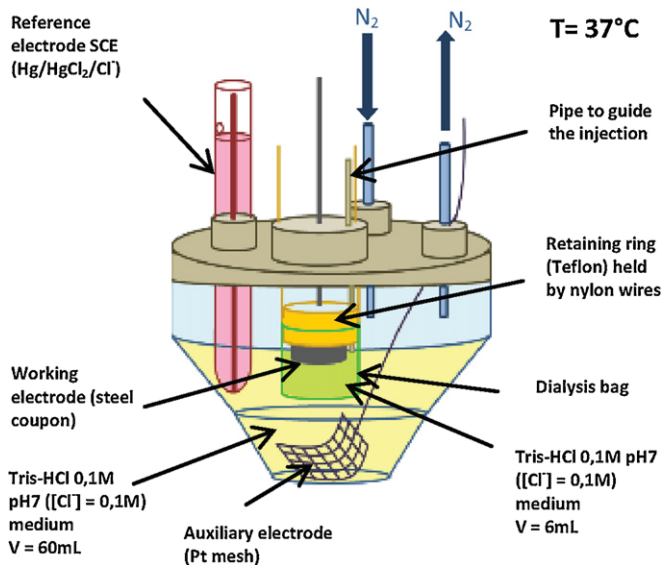


Fig. 1. Scheme of the experimental setup 2 with a dialysis bag.

cell-free culture medium, the formation rate of H_2 was more than 5 times higher (274 ± 49 nmol eeq/h). Thus, hydrogenases released from cells could be adsorbed on the Fe surface and, by direct electron transfer, could catalyse the H_2 formation. In their natural environment, release of hydrogenases in the medium by some microorganisms has been suggested to be accidental or to take place with the purpose of producing the small compounds required for the catabolism of others: development thanks to a sacrificial sub-population [3]. Thus, the impact of microorganisms (such as IRB or SRB) on the corrosion process [23,24] could be directly due to the involvement of hydrogenases as free enzymes in solution rather than occurring only inside cells as was suspected so far [25]. The free hydrogenases could adsorb to an electron donor surface to catalyse the formation of H_2 and thus the corrosion process.

Because of their excellent properties (high efficiency, high specificity, low over-potential for H_2 oxidation, biodegradability), hydrogenases are emerging as good candidates in many processes, notably in biofuel cells. Hydrogenase coated electrodes have been investigated [21,26,27], often using a graphite-based electrode [27–30]. These technologies are also based on the idea that hydrogenases could be adsorbed on the surface of electrodes and could take electrons directly from conductive materials at this surface to catalyse the formation of H_2 . Lukey et al. [28] adsorbed two different hydrogenases from *Escherichia Coli* as a film on a pyrolytic graphite edge electrode (at pH6, 30 °C) and showed that they were able to catalyse electrochemical reactions that usually required a large overpotential. But the efficiency of these coated electrodes is very limited, notably due to the inactivation of the hydrogenases because of the protein desorption [26] and/or deactivation/conformation change [30]. A new strategy is being explored to better immobilize hydrogenases on the electrode surface by orienting them [26,30].

Among the hydrogenases ([Ni-Fe]-hydrogenases, [Fe-Fe]-hydrogenases, [Ni-Fe-Se]-hydrogenases), [Fe-Fe]-hydrogenases were chosen for the present study because of their high activity in the reduction of protons (10- to 100-fold that of [Ni-Fe]-hydrogenases) [31]. [Fe-Fe]-hydrogenases, often found as monomers, contain a catalytic domain, called the H-cluster, and a variable number of Fe-S clusters thought to be involved in electron transfer [14,21,32]. The H-cluster of [Fe-Fe]-hydrogenase is composed of a 2Fe subsite covalently bound to a [4Fe-4S] sub-cluster.

In the present work, the [Fe-Fe]-hydrogenase from *Clostridium acetobutylicum* (*Ca*) was selected, as this bacteria is known to be the microorganism that most efficiently produces hydrogen from hexose [31,33]. Its catalytic domain is an arrangement of six iron atoms in the form of two groups: [4Fe-4S] and [2Fe], where the two iron atoms connected together constitute the active site. After the purification process, the hydrogenase was embedded in a buffered solution with low concentrations of dithionite and desthiobiotin. It has been demonstrated in a previous work that these molecules have an inhibiting effect on the corrosion process [34]. The concentration of the additional molecules, essential for the purification process, was optimized to allow a high activity of hydrogenase and a lower impact on the electrochemical response for corrosion tests simultaneously. While this previous work only studied the effect of additional molecules, the present one focused on the influence of hydrogenase on the anaerobic corrosion of mild steel, using a containment technique (dialysis bag) that concentrated the amount of enzyme around the surface. Electrochemical measurements (open-circuit potential monitoring, polarisation resistance, impedance and cathodic electrolysis) and surface and medium analysis were used to decipher the hydrogenase action in chloride neutral medium.

2. Materials and methods

2.1. Hydrogenase production and purification

Tris(hydroxymethyl) aminomethane (named Tris) was purchased from Acros Organic, and hydrochloric acid, sodium dithionite and desthiobiotin were from Sigma. The Tris-HCl medium was prepared in order to have a final concentration of 0.1 M of Tris in distilled water. The pH was adjusted to pH7 or pH8 by adding concentrate HCl solution and using mechanical stirring. Once the pH had stabilized, the Cl^- concentration was adjusted to 0.1 M using KCl.

The hydrogenases in this work were [Fe-Fe]-hydrogenases. They are not commercialized and were produced, extracted and purified from *Clostridium acetobutylicum* cells in a 0.1 M pH8 Tris-HCl medium at INSA, Toulouse. The purification process used and the measurement of their oxidation activity were as described in [35,36].

At the end of the purification process, no dithiothreitol (DTT) was added to the fraction of interest, thus avoiding the “polluted” effect for the electrochemical study of hydrogenase, as shown in a previous work [34]. The pure [Fe-Fe]-hydrogenase was recovered in a 0.1 M Tris-HCl medium containing dithionite and desthiobiotin at low concentrations. The hydrogenase solution was divided into aliquots, flushed with pure hydrogen and stored at 4 °C. The specific activities (measured on the day of injection into the electrochemical cell), concentrations and compositions of the hydrogenase solutions used in this work are reported in Table 1. Specific activities represent the catalytic activity per unit mass of protein (U/mg of enzyme).

Hydrogenase solutions 1 and 2 were from the same purification fraction. Hydrogenase solution 3 was derived from another purification fraction with an optimized composition of additional molecules (dithionite and desthiobiotin) [34].

2.2. Electrochemical cell setup

The experiments were performed with a three-electrode system in closed cells (Metrohm).

The working electrodes were 2-cm-diameter cylinders of S235JR mild steel from Descours-Cabaud, France (elemental composition by weight percentage: Fe balance, 0.17C, 1.4Mn, 0.55Cu, 0.03S,

Table 1

Compositions of hydrogenase solutions used.

		Tris-HCl	dithionite	desthiobiotin	hydrogenase		Specific activity
					concentration		
Hydrogenase solution in the aliquot	1	0.1 M pH 8 [NaCl]=0.15 M	0.5 mM	10 mM	290 µg/mL	4.39 µM	2700 U/mg
	2	0.1 M pH 8 [NaCl]=0.15 M	0.5 mM	10 mM	290 µg/mL	4.39 µM	2570 U/mg
	3	0.1 M pH 8 [NaCl]=0.15 M	0.5 mM	7.5 mM	137 µg/mL	2.07 µM	4400 U/mg

0.03P, 0.01N). They were surrounded by adhesive-lined heat shrink tubing (His-A 24/8 PO-X-BK) from HellermannTyton, leaving a flat disk of the surface uncovered, with a total exposed area of 3.14 cm². The electrical connection was provided by a titanium threaded rod also protected with heat shrink tubing. Coupons were successively ground using SiC papers with increasingly fine grit (P120 to P2400) and then rinsed with distilled water and stored for 24 h before the experiments began.

Saturated calomel electrodes (SCE) from Materials Mates Sentek were used as references and platinum (Pt, 10% Ir) meshes, connected with platinum (Pt, 10% Ir) wire, from Goodfellow, were used as counter electrodes. The Pt electrode was cleaned before use by heating it in the oxidizing flame of a gas burner.

The electrodes were immersed in 0.1 M pH7 Tris-HCl medium containing 0.1 M Cl⁻. The choice of pH7 was a compromise between the pH8 of the purification process and pH6.3, which is the optimum for hydrogenase towards the hydrogen production [37].

The electrochemical cell was hermetically closed and the temperature was maintained at 37 °C by means of a water-bath. Nitrogen was continuously bubbled into the solution for 1 h before the immersion of the working electrodes. After the deoxygenation, the steel coupon was submerged in the solution and the nitrogen flow was maintained above the solution surface throughout the experiment. After 1 h and 15 min, hydrogenase solution or control solutions were injected with a syringe (Hamilton) in strict anaerobic conditions, oxygen having been removed from the syringe with nitrogen. Firstly, in setup 1, the hydrogenase solutions (or controls) were injected in the whole volume of the electrochemical cell (60 mL) as described in [34]. A second experimental setup (setup 2) that concentrated the hydrogenase around the working electrode by using a closed regenerated cellulose tubular membrane (also called a dialysis bag) was tested (Fig. 1). The porosity (nominal MWCO: 12000–14000) of the dialysis bag was chosen such that hydrogenase remained inside it while the other chemicals (particularly dithionite and desthiobiotin) in the electrochemical cell could leave. The hydrogenase solutions (and controls) were injected into the dialysis bag containing 6 mL of 0.1 M pH7 Tris-HCl medium and the concentration of hydrogenase attained was 10 times higher than in the previous experimental setup.

2.3. Electrochemical measurements

The electrochemical measurements were performed by using a VMP2 multipotentiostat (Bio-Logic, SA) monitored by EC-lab 9.98 software.

2.3.1. Open-circuit potential or free corrosion potential

The open-circuit potential (E_{oc}) was monitored versus time for 24 h from the time when the steel coupon was immersed in the solution.

2.3.2. Linear polarisation measurement

Linear polarisation measurement were performed around the open-circuit potential from E_{oc} to $E_{oc} - 20$ mV to $E_{oc} + 20$ mV, at 0.167 mV/s. Polarisation curves were plotted just before the injection; after the injection at 10 min, 30 min and every 30 min up to 5 h; and then at 24 h. Care was taken to be sure that the linear

polarisation measurement did not change the surface state of the steel coupons: evolution of E_{oc} was not affected by performing these measurements. The slope of the polarization curve in the vicinity of the corrosion potential (dj/dE)_{ECorr}, for reactions under activation control, is proportional to the corrosion rate (which is proportional to the corrosion current density) and corresponds to the inverse of the polarisation resistance (R_p) [38,39] as described by Eq. (2).

$$j_{corr} = \frac{B}{R_p} = B \left(\frac{dj}{dE} \right)_{E_{corr}} \quad (2)$$

The proportionality constant, B, for a particular system can be determined empirically (calibrated from separate weight loss measurements for example) or using Tafel curves and the anodic and cathodic slopes. Here B was not determined, just the parameter $1/R_p$ was calculated and was used to evaluate the evolution of the corrosion rate during the immersion in presence or absence of hydrogenase. In order to avoid damaging the electrode surface state by the electrochemical measurement, no Tafel curve was drawn (as the overpotentials needed would have been too high). In practice, slopes ($1/R_p$) were obtained by using the linear part around E_{oc} , i.e., at least from -10 mV/ E_{oc} to $+10$ mV/ E_{oc} .

2.3.3. Impedance

EIS measurements were performed just before the injection, and 5 h and 24 h after the injection. Electrochemical impedance diagrams were drawn at E_{oc} with a frequency range from 100 kHz to 10 mHz, 10 points per decade and an amplitude of 10 mV peak to peak. The impedance was modelled using EC-lab[®] software.

2.3.4. Electrolysis

Electrolysis was carried out at a cathodic potential of -0.1 V vs E_{oc} .

2.4. Surface analysis, imaging and medium analysis

Metal deterioration was assessed by Scanning Electron Microscopy (SEM) and surface chemical analysis was performed by Energy Dispersive X-ray analysis (EDX) using a MEB-FEG Jeol JSM7100F TTLS – TM 3000 with a working distance of 10 mm and an acceleration voltage of 15 kV. For each sample, many measurements (at least three) were performed at different spots on the sample surface. For some coupons, the surface of the mild steel was cleaned of corrosion products by placing the coupon in a solution containing 50% vol. HCl and 2.5 g/L EDTA for 30 s.

The Nital metallographic attack was carried out by soaking the mild steel coupon in a 97% ethanol/3% nitric acid solution for 2 min.

Total dissolved iron found in the medium at the end of the experiments was measured by Inductively Coupled Plasma Spectroscopy (ICP-Spectroscopy, JY Ultima).

Table 2
Final concentrations obtained in the electrochemical cell for experimental setup 1 and in the dialysis bag for experimental setup 2, just after the injection and potential ennoblement (ΔE) observed in the two setups in presence of hydrogenase at various times, from Fig. 2, for S235JR mild steel electrodes.

Setup	Solution injected	Injected volume	Hydrogenase in the electrochemical cell/dialysis bag just after injection		$\Delta E = E_{oc}(t) - E_{oc}(t=0)$ (mV) at different times (h)				
			Concentration	Specific activity (U/mL)	t = 0.17	t = 0.5	t = 1.1	t = 4.7	t = 24
Setup 1 Classical electrochemical cell	Hydrogenase solution 1	7.5 μ L	0.5 nM	9.8×10^{-2}	0 \pm 0	-1 \pm 0	-2 \pm 0	-3 \pm 0	6 \pm 0
		75 μ L	5.5 nM	9.8×10^{-1}	15 \pm 4	18 \pm 6	19 \pm 8	15 \pm 7	14 \pm 6
Setup 2 Dialysis bag	Hydrogenase solution 2	7.5 μ L	5.5 nM	9.3×10^{-1}	1 \pm 1	3 \pm 1	3 \pm 4	4 \pm 5	17 \pm 8
		75 μ L	54.9 nM	9.3	46 \pm 1	50 \pm 1	49 \pm 1	36 \pm 1	29 \pm 1
		150 μ L	109.8 nM	18.6	49 \pm 3	55 \pm 2	54 \pm 1	51 \pm 1	51 \pm 3
	Hydrogenase solution 3	160 μ L	54.9 nM	16.1	36 \pm 2	44 \pm 3	45 \pm 2	42 \pm 2	48 \pm 4

Table 3
Variation in time of impedance parameters corresponding to E_{oc} measurement from Fig. 4, for S235JR mild steel electrodes. Injection of control solution at $t=0^+$. R_s = solution resistance, R_1 and R_2 = resistances corresponding to the circle diameters at HF and MF respectively; Q_1 , α_1 and Q_2 , α_2 = characteristic parameters of CPE at HF and MF respectively; C_1 and C_2 = capacitances calculated at HF and MF respectively; δ = thickness of the oxide film.

t (h)	R_s (Ω cm ²)	High Frequency domain (HF)					Medium Frequency domain (MF)				
		R_1 (Ω cm ²)	Q_1 (F.s α^{-1})	α_1	C_1 (μ F/cm ²)	δ (nm)	R_2 (Ω cm ²)	Q_2 (F.s α^{-1})	α_2	C_2 (μ F/cm ²)	
0	67	47	1.1×10^{-4}	0.8	8	136	1367	1.2×10^{-3}	0.7	129	
5	63	28	8.6×10^{-5}	0.8	6	173	8959	3.9×10^{-4}	0.8	41	
24	71	15	5.9×10^{-5}	0.9	6	166	11754	4.0×10^{-4}	0.7	27	

3. Results and discussion

3.1. Evolution of E_{oc} in classical electrochemical cell and in dialysis bag setups

Mild steel (S235JR) coupons were immersed in a 0.1 M pH7 Tris-HCl (0.1 M Cl⁻) medium for 24 h. After a stabilization of the free potential for 1 h and 15 min, hydrogenase solutions were injected in strictly anaerobic conditions ($t=0^+$). Experiments were performed in the two setups described in part 2.2: volumes of 7.5 μ L up to 160 μ L of the enzymatic solutions, the characteristics of which are given in Table 1, were injected; the enzyme concentrations (range 0.5–109 nM) and activities (range 9.8×10^{-2} –18.6 U/mL) inside the classic electrochemical cell and in the dialysis bag, immediately after the injection, are reported in Table 2. Each hydrogenase experiment was associated with a control experiment performed by injecting the control solution without hydrogenase (containing 0.1 M Tris-HCl, dithionite and desthiobiotin).

The variation of the open-circuit potential (E_{oc}) was recorded versus time for 24 h (Fig. 2) and typical curves obtained for each volume injected are presented. Potential ennoblement values (ΔE) were calculated by subtracting the starting potential, just before the injection, from the value of the potential at a given time, and the average, obtained for each injected volume, is reported in Table 2. The injection process did not introduce oxygen into the cell since the injection of deoxygenated 0.1 M pH7 Tris-HCl medium induced no evolution of the E_{oc} , as shown in a previous work [34].

All the injections of hydrogenase, in both experimental setups (except for the injection of a volume of 7.5 μ L), induced a potential jump (as shown in Fig. 2 and Table 2), whereas a potential fall was observed in the first hours after the injection of the corresponding control solutions as demonstrated in [34].

The injection of 7.5 μ L of hydrogenase solution, as for the corresponding control solution, induced no significant evolution of E_{oc} in either setup (Fig. 2(a) and (b)), even with a tenfold higher concentration of hydrogenase in setup 2 (Table 2). Moreover, the injection of 7.5 μ L in setup 2, which should have given an enzyme concentration equivalent to that obtained with a 75 μ L injection in setup 1 (Table 2), was not sufficient to lead to the same evolution of the E_{oc} .

In contrast, the injection of higher volumes (75 μ L of hydrogenase solution) induced a potential ennoblement in both setups, reaching a maximum after around 1 h (Fig. 2(a) and (b)); the ennoblement was greater in setup 2 (49.5 mV) than in setup 1 (19.5 mV). This observation suggests that the amount of hydrogenase (54.9 nM in setup 2 instead of 5.5 nM) had an important impact on the E_{oc} and, ultimately, on the corrosion process. Otherwise, the further E_{oc} decrease could be explained by the desorption/deactivation of hydrogenase. Doubling the injected volume (150 μ L instead of 75 μ L) in setup 2 (Fig. 2(b)) induced the same potential jump, which, however, remained stable until the end of the experiment ($\Delta E = 50.5$ mV after 24 h). A reserve of enzyme in solution could certainly counteract the desorption/deactivation of hydrogenase on the mild steel surface. In addition, the injection of 160 μ L of hydrogenase solution 3 in setup 2 (Fig. 2(c)) also induced a potential ennoblement equivalent to that with 75 μ L of hydrogenase solution 2 in setup 2 ($\Delta E = 44.5$ mV after 1 h). This is in accordance with their hydrogenase concentrations, which were equal (as shown in Table 2). However, with an activity two times higher, the potential remained stable over time with 160 μ L of hydrogenase solution 3 ($\Delta E = 47.5$ mV after 24 h), unlike what was observed with 75 μ L hydrogenase solution 2 (Fig. 2(b)). In fact, the evolution of E_{oc} for 160 μ L hydrogenase solution 3 and 150 μ L hydrogenase solution 2 was equivalent despite a two times lower concentration, but the specific activity was the same. Thus, the increase of enzyme concentration is not the only parameter that plays a role in exacerbating the corrosion process: activity also has a major influence.

To support the observations concerning E_{oc} evolution, linear polarisation measurements were performed in the vicinity of E_{oc} to evaluate the polarisation resistance (R_p) and impedance experiments were carried out to understand the global behaviour of the interface in presence of hydrogenase.

3.2. Evolution of $1/R_p$ in electrochemical cell and in dialysis bag setups

During the 24 h immersion, linear polarisation measurements were performed in the vicinity of E_{oc} at different times (just before the injection, at 10 min and 30 min after the injection, then every 30 min until 5 h after injection and then at 24 h). Fig. 3 shows two

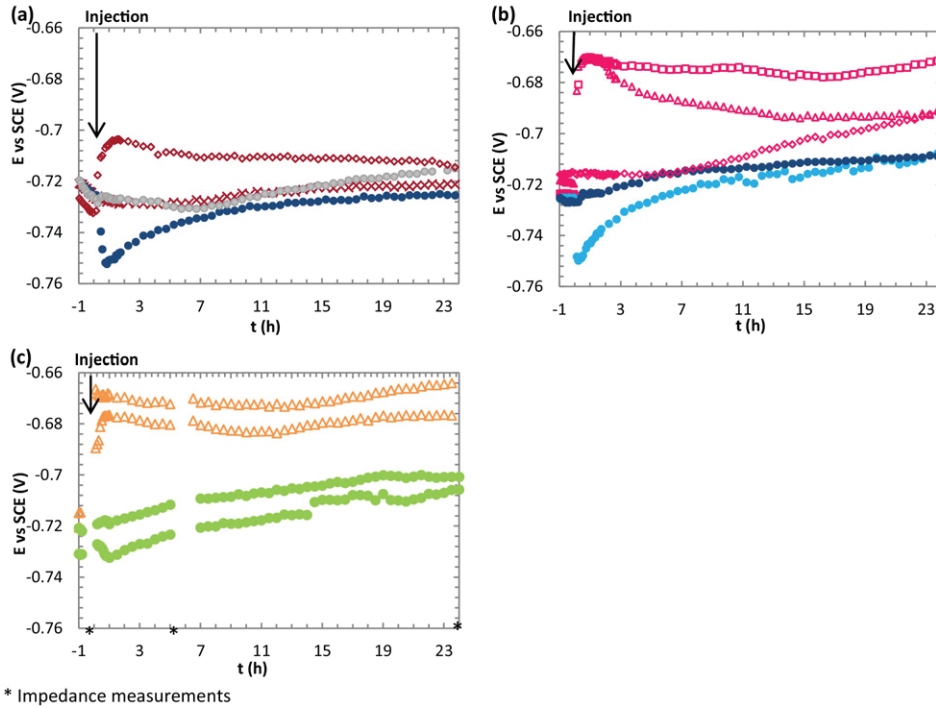


Fig. 2. Open-circuit potential (E_{oc}) versus time for S235JR mild steel electrodes in 0.1 M pH7 Tris-HCl medium. Injection at $t=0^+$ of solution with or without hydrogenase. (a) Setup 1: \times 7.5 μ L hydrogenase solution 1, \diamond 75 μ L hydrogenase solution 1, \bullet 7.5 μ L control solution, \bullet 75 μ L control solution. (b) Setup 2: \diamond 7.5 μ L hydrogenase solution 2, \triangle 75 μ L hydrogenase solution 2, \square 150 μ L hydrogenase solution 2, \bullet 7.5 μ L control solution, \bullet 75 μ L control solution. (c) Setup 2: \triangle 160 μ L hydrogenase solution 3, \bullet 160 μ L control solution. (For interpretation of the references to colour in this figure legend, the reader is referred to the web version of this article.)

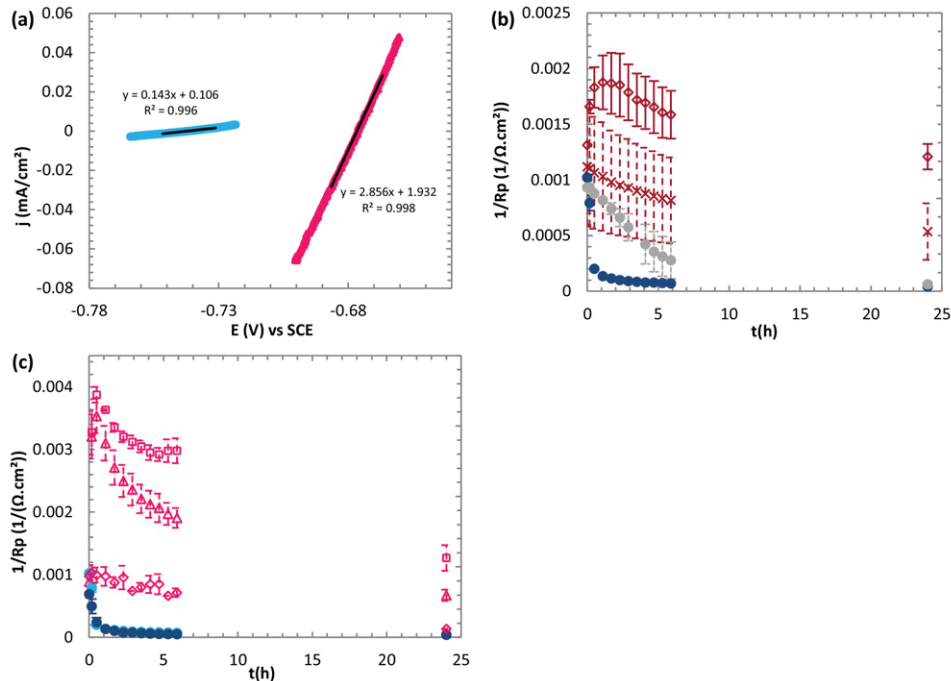


Fig. 3. Determination and evolution in time of the inverse of polarisation resistance ($1/R_p$) for S235JR mild steel electrodes in 0.1 M Tris-HCl pH7 medium. Injection at $t=0^+$ of solution with or without hydrogenase. (a) Examples of polarisation curves to determine $1/R_p$ (slope of the curve), obtained in setup 2 after 10 min of immersion with: \triangle 75 μ L hydrogenase solution 2, \bullet 75 μ L control solution. (b) $1/R_p$ versus time for experiments performed in setup 1: \times 7.5 μ L hydrogenase solution, \diamond 75 μ L hydrogenase solution, \bullet 7.5 μ L control solution, \bullet 75 μ L control solution. (c) $1/R_p$ versus time for experiments performed in setup 2: \diamond 7.5 μ L hydrogenase solution 2, \triangle 75 μ L hydrogenase solution 2, \square 150 μ L hydrogenase solution 2, \bullet 7.5 μ L control solution, \bullet 75 μ L control solution. (For interpretation of the references to colour in this figure legend, the reader is referred to the web version of this article.)

examples of the curves obtained (Fig. 3(a)) and the evolution in time of the inverse of R_p ($1/R_p$ in Fig. 3(b) and (c)). $1/R_p$ corresponds to the slope obtained on the linear part of the polarisation curves around E_{oc} , and indicates the evolution of the corrosion rate corresponding to the E_{oc} evolution recorded in Fig. 2(a) and (b).

The $1/R_p$ starting value was the same in all cases, around $1 \times 10^{-3} \text{ 1}/(\Omega \text{ cm}^2)$, indicating that the experiments were repeatable. Injecting the control solution always led to a fast decrease of $1/R_p$. After 24 h, $1/R_p$ had been divided by 15 for the control in setup 1 ($6.4 \times 10^{-5} \text{ 1}/(\Omega \text{ cm}^2)$) and by 20 in setup 2 ($4.2 \times 10^{-5} \text{ 1}/(\Omega \text{ cm}^2)$). As identified in a previous work [34], dithionite and desthiobiotin seemed to have an inhibiting effect (inhibitor reaction occurring at the surface of mild steel for dithionite, mask effect for desthiobiotin) on the corrosion process by decreasing the $1/R_p$ and the E_{oc} .

In contrast, in presence of hydrogenase, $1/R_p$ was always higher than for the corresponding controls. The injection of $7.5 \mu\text{L}$ of hydrogenase solution 1 induced no significant evolution of $1/R_p$ in either setup (as was observed for E_{oc} in Fig. 2). Actually, the values of $1/R_p$ and their evolution corresponded to values obtained in 0.1 M pH7 Tris-HCl medium alone (curves not shown, refer to [34]). However, for the associated control solution, $1/R_p$ decreased. Thus, the volume of $7.5 \mu\text{L}$ was not sufficient to lead to any impact of hydrogenase on the evolution of E_{oc} but was enough for a difference to be observed on the evolution of the corrosion rate.

The injection of $75 \mu\text{L}$ of hydrogenase solution in both setups induced a fast increase of $1/R_p$, reaching a maximum in less than an hour. The increase was greater in setup 2 ($3.5 \times 10^{-3} \text{ 1}/(\Omega \text{ cm}^2)$) than in setup 1 ($1.7 \times 10^{-3} \text{ 1}/(\Omega \text{ cm}^2)$). This observation confirmed a fast increase of the corrosion rate in presence of hydrogenase, which was emphasized by confining the enzyme in a small volume (in the dialysis bag). The maximum of $1/R_p$ was 4.8 times higher in setup 2, while the concentration was ten times higher, suggesting that it was not only the concentration of enzyme that played a role in the corrosion process between hydrogenase and mild steel. Moreover, $1/R_p$ decreased over time to reach a value near the starting ones after 24 h ($9.5 \times 10^{-4} \text{ 1}/(\Omega \text{ cm}^2)$ in setup 1 and $6.7 \times 10^{-4} \text{ 1}/(\Omega \text{ cm}^2)$ in setup 2). Thus, it was confirmed that the impact of hydrogenase on the corrosion process was an immediate effect that did not persist in time, maybe due to desorption of the enzyme and/or its deactivation by a change in the conformation and/or a change of the active surface area.

Doubling the injected volume ($150 \mu\text{L}$) in setup 2 (Fig. 3(b)) induced a similar evolution of $1/R_p$ (fast increase and decrease after half an hour) with a maximum of $3.9 \times 10^{-3} \text{ 1}/(\Omega \text{ cm}^2)$, which was only 1.1 times the value with $75 \mu\text{L}$ of hydrogenase solution 2 in setup 2. However, even though the factor was only 1.1, the decrease of $1/R_p$ was less abrupt, certainly because of an enzyme excess in solution and/or a higher total activity.

3.3. Impedance experiments in dialysis bag setup

Impedance experiments were carried out at E_{oc} in 0.1 M pH7 Tris-HCl medium with or without hydrogenases, just before the injection, at $t = 5 \text{ h}$ and at $t = 24 \text{ h}$. Experiments were conducted in experimental setup 2 with $160 \mu\text{L}$ hydrogenase solution 3 or control solution, during the E_{oc} monitoring (Fig. 2(c)). Fig. 4 shows the impedance response of the mild steel electrode exposed to Tris-HCl medium with an injection of the control solution at $t = 0^+$. On the Nyquist diagrams (global and zoom, Fig. 4(a) and (b)), two to three phenomena can be identified. At high frequencies (HF: $100 \text{ kHz} - 1 \text{ kHz}$) there is a semi-circle with a small diameter (Fig. 4(b)) that decreases with time. At medium frequencies (MF: $1 \text{ kHz} - 1 \text{ Hz}$) the depressed semi-circle obtained before injection becomes a large semi-circle that flattens at low frequencies (LF: $1 \text{ Hz} - 10 \text{ MHz}$) corresponding to two phenomena. The plots of the

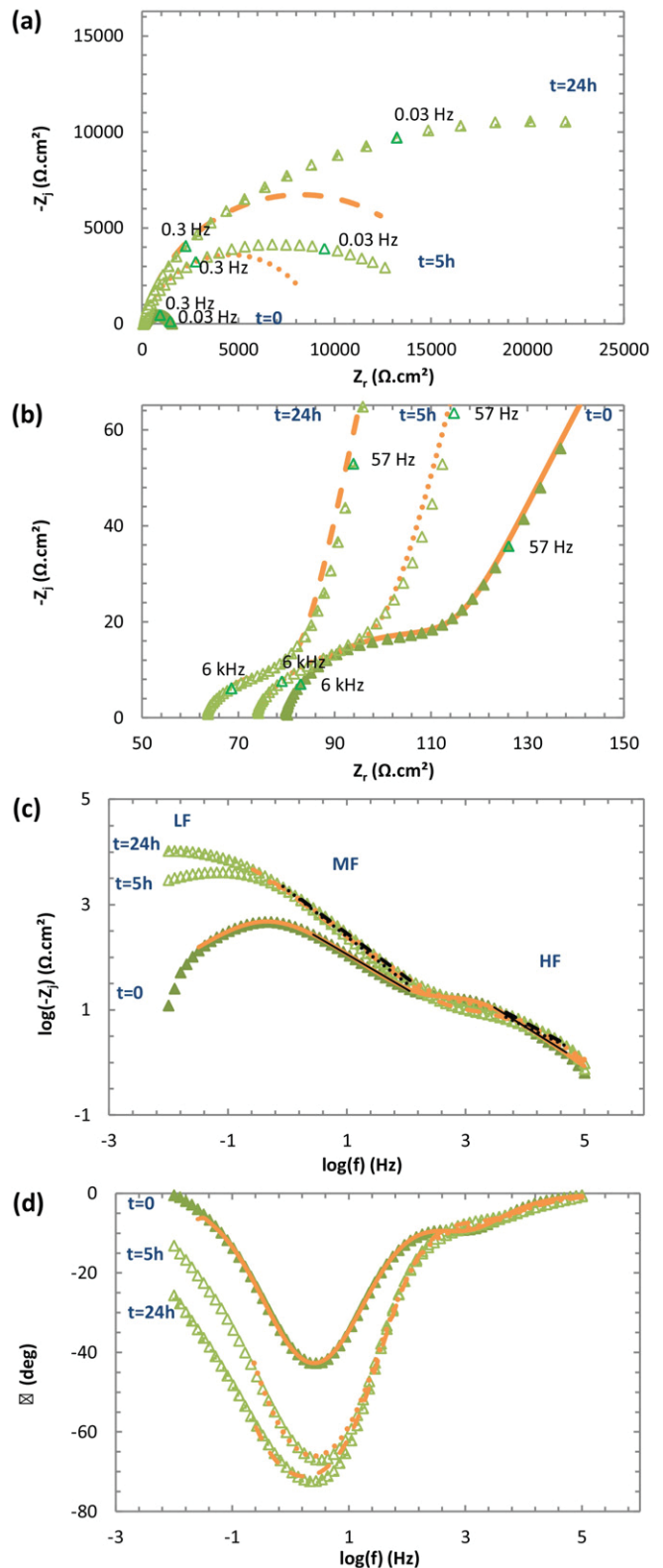


Fig. 4. Impedance diagrams of S235JR mild steel electrodes plotted at E_{oc} at \blacktriangle $t = 0$ (just before the injection) ($E_{oc} = -0.721 \text{ V vs SCE}$), \triangle $t = 5 \text{ h}$ ($E_{oc} = -0.717 \text{ V vs SCE}$) and \blacktriangle $t = 24 \text{ h}$ ($E_{oc} = -0.707 \text{ V vs SCE}$) in 0.1 M Tris-HCl pH7 medium. Corresponding fitted lines are represented by orange: solid, dotted and dashed lines, respectively; using the electrical model reported in Fig. 5 and the parameter values of Table 3. Injection of $160 \mu\text{L}$ control solution in the dialysis bag at $t = 0^+$. (a) Nyquist plot, (b) Nyquist zoom-in, (c) log imaginary modulus vs log frequency, (d) Bode phase angle vs log frequency. (For interpretation of the references to colour in this figure legend, the reader is referred to the web version of this article.)

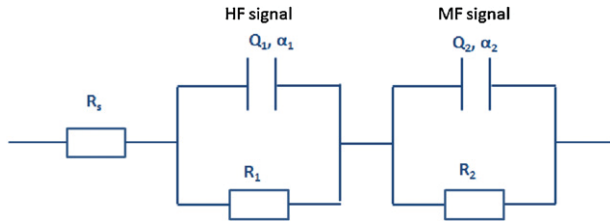


Fig. 5. $R_s + Q_1//R_1 + Q_2//R_2$ electric model to fit the two distinct semi-circles observed on the Nyquist plot. R_s = solution resistance, R_1 and R_2 = resistances corresponding to the circle diameters at HF and MF respectively; Q_1, α_1 and Q_2, α_2 = characteristic parameters of CPE at HF and MF respectively.

imaginary modulus and Bode phase angle vs. frequency (Fig. 4(c) and (d)) confirm the occurrence of these two/three phenomena. As the phenomenon at LF was not well-defined, only the phenomena at HF and MF were characterized quantitatively. For this, the $R_s + Q_1//R_1 + Q_2//R_2$ model was used (Fig. 5), where R_s is the electrolyte resistance, Q_1, α_1 (characteristics of a Constant Phase Element [40]) and R_1 are the parameters corresponding to the small depressed circle at HF, and Q_2, α_2 and R_2 are those corresponding to the depressed semi-circle at MF.

The values of the impedance parameters (detailed in Supplementary information) are brought together in Table 3. Throughout the immersion test, R_s remained stable ($63\text{--}71 \Omega \text{ cm}^2$).

At HF, the small resistance values obtained ($15\text{--}47 \Omega \text{ cm}^2$), especially when the immersion time increased, suggest that the HF phenomenon was related to the presence of oxides on the steel surface. The capacitance C_1 was then calculated using the power-law distribution as proposed by Hirschorn et al. [41,42] (Supplementary information). This method of calculation is preferred in the case of a normal distribution of resistivity and provides the most accurate assessment of CPE parameters in terms of physical properties [43] for diverse systems such as aluminium oxides, oxides on stainless steel, etc. The capacitance was calculated to be around $6\text{--}8 \mu\text{F}/\text{cm}^2$. Then the thickness of the oxide film can be estimated using the following equation:

$$\delta = \frac{\varepsilon \varepsilon_0}{C} \quad (3)$$

with ε_0 the vacuum permittivity, equal to $8.85 \times 10^{-14} \text{ F}/\text{cm}$, and ε the permittivity inside the oxide, equal to 12, which is the number habitually used for iron oxides [44]. Before the injection, the thickness of the oxide layer was evaluated at 136 nm. After injection it increased a little to reach 173 nm after 5 h, and remained stable thereafter (166 nm after 24 h).

At MF, linear parts were observed on the plot of the modulus of the imaginary component of the impedance vs. the frequency in logarithmic coordinates (Fig. 4(c)). The slope values of these linear parts were used to determine α_2 values in order to confirm whether the system had a constant phase element (CPE) behaviour or purely capacitive behaviour [45–47]. For all instants, the α_2 values were found to be lower than 1, confirming a CPE behaviour, i.e. the system exhibited a heterogeneous distribution of time constants. The effective capacitances associated with the CPE were calculated using Brug's equation [48] (Supplementary information). The capacitance decreased after the injection of the control solution and over time to reach $27 \mu\text{F}/\text{cm}^2$ after 24 h. These values of capacitance correspond to double layer capacitance values (classically in the range of $10\text{--}100 \mu\text{F}/\text{cm}^2$ [45]). Thus it can be assumed that the CPE behaviour was due to a surface distribution of time constants linked to the charge transfer. Consequently, the diameter, R_2 , of the depressed semi-circles can be attributed to a charge transfer resistance (R_{ct}), which increased radically after the injection of the control solution (10 times the initial value). Consequently, as the surface of mild steel was more resistive or less reactive, the corro-

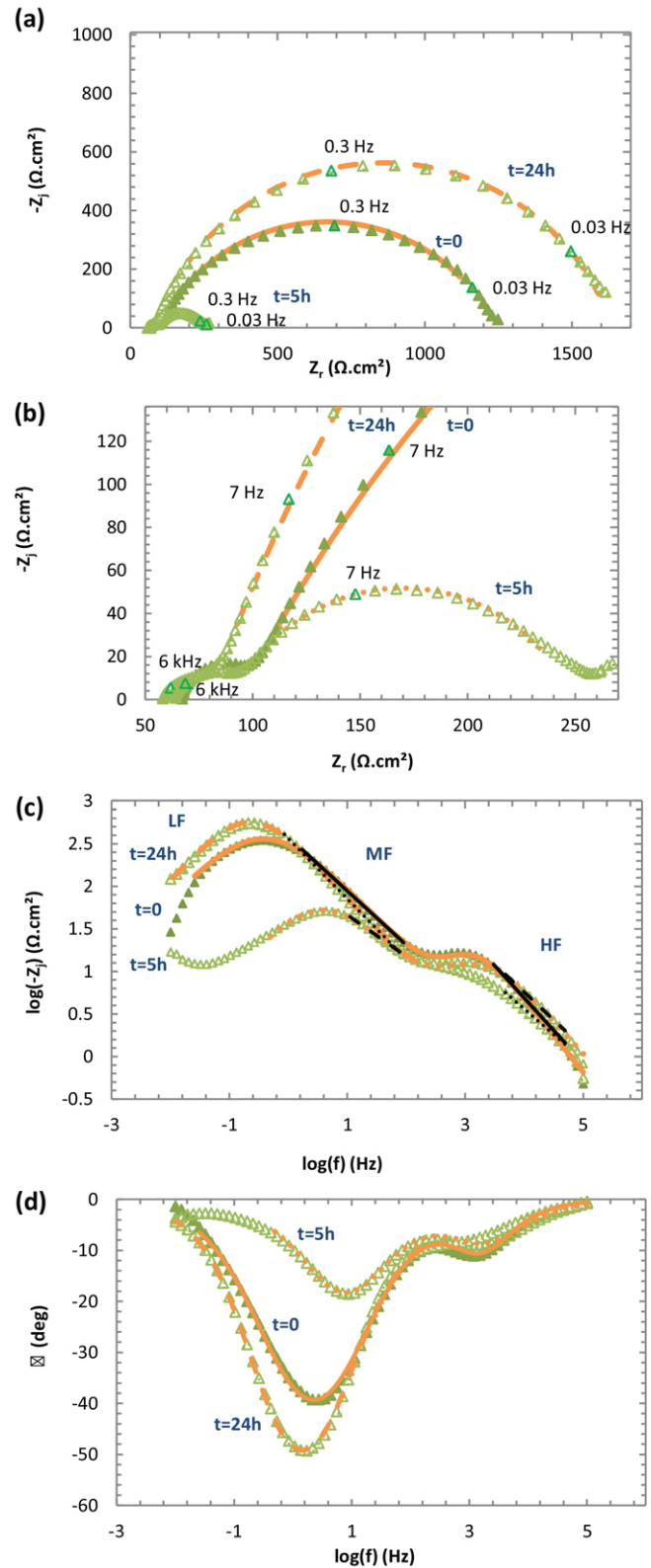


Fig. 6. Impedance diagrams of S235JR mild steel electrodes plotted at E_{oc} at \blacktriangle $t=0$ (just before the injection) ($E_{oc} = -0.722 \text{ V vs SCE}$), \triangle $t=5 \text{ h}$ ($E_{oc} = -0.682 \text{ V vs SCE}$) and \blacktriangle $t=24 \text{ h}$ ($E_{oc} = -0.679 \text{ V vs SCE}$) in $0.1 \text{ M Tris-HCl pH7}$ medium. Corresponding fitted lines are represented by orange: solid, dotted and dashed lines, respectively; using the electrical model reported in Fig. 5 and the parameter values of Table 4. Injection at $t=0^*$ of $160 \mu\text{L}$ HydA solution 3 in the dialysis bag. (a) Nyquist plot, (b) Nyquist zoom-in, (c) log imaginary modulus vs log frequency, (d) Bode phase angle vs log frequency. (For interpretation of the references to colour in this figure legend, the reader is referred to the web version of this article.)

sion rate decreased, which confirms the R_p results with only 75 μL of control solution (Fig. 3).

In presence of hydrogenase, as can be seen in the Nyquist plot (Fig. 6(a) and (b)), two to three phenomena also occurred. The impedance signal before injection (Fig. 6) was the same as for the control solution (Fig. 4), which indicates the reproducibility for the initial conditions. At HF, a small semi-circle was observed at any time as in the control solution. At MF, the diameter of the depressed semi-circle obtained before injection decreased drastically at 5 h and then it returned to around the initial plot after 24 h. At LF, the depressed semi-circle evolved as another phenomenon (not well identified) occurred. The plot of the imaginary modulus and Bode phase angle vs frequency (Fig. 6(c) and (d)) confirmed the occurrence of these two/three phenomena, especially at 5 h.

The same model was used (as for control solution, Fig. 5) to quantify R_s and the parameters corresponding to the small circle (HF) and the depressed semi-circle (MF). The values of the impedance parameters are given in Table 4.

Values of α_1 and α_2 were found to be lower than 1, indicating a CPE behaviour for both semi-circles at HF and MF. During the experiment, R_s remained stable (58–66 Ωcm^2). At HF, the resistances estimated were small (24–29 Ωcm^2) and the capacitances were in the range of 4–9 $\mu\text{F}/\text{cm}^2$. Thus the HF semi-circle could be attributed to an oxide layer developing on the surface of the mild steel (as in control conditions). The film thickness was estimated using Eq. (3) and tended to decrease with the immersion time, to reach half the initial thickness.

At MF, capacitances calculated with Brug's equation were in the high range of a double layer capacitance and increased with time to reach 210 $\mu\text{F}/\text{cm}^2$ after 24 h. The SEM images of cross sections of mild steel after 24 h of immersion with or without hydrogenases, reported in Fig. 7, show a noteworthy difference of the surface of the mild steel. Without hydrogenase, the surface seemed smoother than with hydrogenases. Besides corrosion pitting (with a depth of up to 10 μm), the surface was rougher and more damaged in presence of hydrogenase. Consequently, in presence of enzyme, the capacitance values were most probably overestimated, and even more so with time, since the active surface was larger (due to the increased roughness) than the geometric surface (considered in the calculations).

Considering that the values of capacitances corresponded to double layer capacitance values, R_2 could be attributed to an R_{ct} that decreased drastically (by a factor of 7 after 5 h). These findings confirm that the corrosion rate was increased after the injection of hydrogenase (Fig. 3). After 24 h of immersion, the resistance was again equivalent to the initial value.

To sum up, in both media the steel/electrolyte interface was described by an oxide layer on which more or less charge transfer occurred, depending on the presence or absence of hydrogenase. A third phenomenon was also observed at low frequency, but it was not sufficiently well-defined to be correctly exploited. After 5 h of immersion in presence of hydrogenase, the charge transfer resistance had decreased markedly. The surface of the mild steel was therefore more reactive, less resistant, even after the installation of a saturation plateau of E_{oc} (Fig. 2(c)). Impedance tests also confirmed that the impact of hydrogenase on the corrosion of mild steel occurred not only at the very beginning of the experiment but could take several hours since R_{ct} was still lower than its starting value at $t = 5$ h. After 24 h, although the impedance plot was equivalent to the starting one, the capacitance was higher, confirming an active surface that was larger than the geometric surface.

3.4. Surface and medium analysis

SEM images of the electrode surface before immersion 24 h after grinding (Fig. 8(a)) showed that grinding stripes were well defined

Table 5

Fe concentration determined by ICP in the dialysis bag and the electrochemical cell, measurement after immersion of mild steel for 24 h in setup 2.

	[Fe] (mg/mL)	
	Dialysis bag	Electrochemical cell
7.5 μL hydrogenase solution 2	9.0	7.3
75 μL hydrogenase solution 2	23.8	24.3
75 μL Control solution	2.8	2.0

before the experiments. After 24 h of immersion in the medium without hydrogenase, grinding stripes were still visible even with the naked eye (Fig. 8(b–c)). This was also the case after the cleaning operation (images not shown), proving that very small amounts of corrosion products were deposited. The EDX analysis (given in Supplementary information) showed a qualitative tendency: globally, a slight decrease occurred in the proportion of Fe due to its dissolution and the formation of an oxide layer.

After 24 h of immersion in presence of hydrogenase, grinding stripes were no longer visible (Fig. 8(d–f)). The surface aspect of the mild steel brought its structure to light: size, shape and number of grains, as could be observed with a 3% Nital metallographic attack (Fig. 9).

Thus, the presence of hydrogenase induced an attack at the grain boundary. Globally, a high Fe dissolution occurred in the presence of hydrogenase (of 10–20% with respect to the initial value) and a preferential enrichment of the other elements present in the composition of the mild steel (C, Mn, Cu), particularly C, the percentage of which tripled (Table in Supplementary information).

Without hydrogenase, numerous pits were observed, principally with round shapes (Fig. 10(a–c)). With the 160 μL control solution, holes were fewer but much bigger (50–80 μm^2) than for the 75 μL control solution. The medium composition and especially the dithionite and desthiobiotin concentrations certainly led to a different surface evolution and thus a different distribution and propagation of pits. In presence of hydrogenase, many pits were observed, mostly with a square shape and often associated with a grain of ferrite (16 μm^2) (Fig. 10(c–g)). A deposit at the pit centre was very often observed and was principally composed of Mn, S and ferrous oxide (Supplementary information). This might suggest that pits were initiated in the surroundings of MnS inclusions that remained at the surface [49].

Solutions in the electrochemical cell and in the dialysis bag were orange after 24 h of immersion in presence of hydrogenase, and even more orange with a higher concentration of hydrogenase (relative to the observations in Figs. 2 (b) and 3 (b)). In contrast, the solution remained colourless until the end for all the control experiments. This observation also confirmed that the corrosion process was enhanced in the presence of hydrogenase. Dissolved Fe concentration was estimated by ICP measurement in both the electrochemical cell and the dialysis bag (Table 5). The Fe concentration was equivalent in the cell and in the dialysis bag, small compounds passing through the membrane. For an enzyme injection volume of 7.5 μL , even with an E_{oc} and a $1/R_p$ that evolved as though no injection had occurred (due to the antagonistic effect of hydrogenase and additional molecules), a dissolution of Fe was observed. In presence of 75 μL hydrogenase solution 2, the dissolution was enhanced. The injection of control solution (75 μL) involved less dissolution of iron than the solution with enzyme. This confirmed the inhibiting effect of additional molecules on the corrosion process, which is consistent with $1/R_p$ decrease.

3.5. Cathodic depolarisation by hydrogenase

Some supplementary electrochemical experiments were performed using a cathodic polarisation (–100 mV vs E_{oc}) (Fig. 11). The

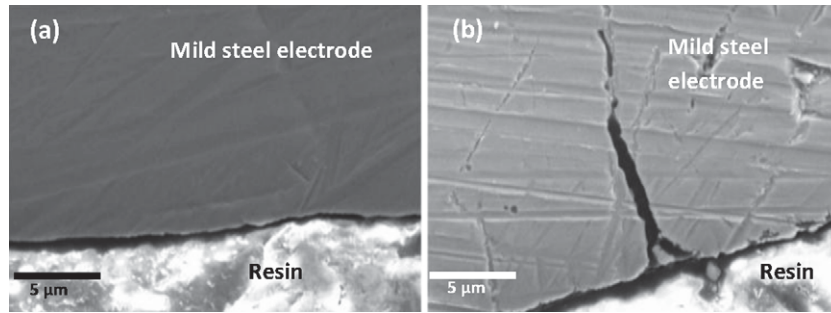


Fig. 7. SEM images of cross section of S235JR mild steel electrode after 24 h of immersion in 0.1 M pH7 Tris-HCl with or without the presence of hydrogenase, (a) 160 μ L control solution, (b) 160 μ L hydrogenase solution 3.

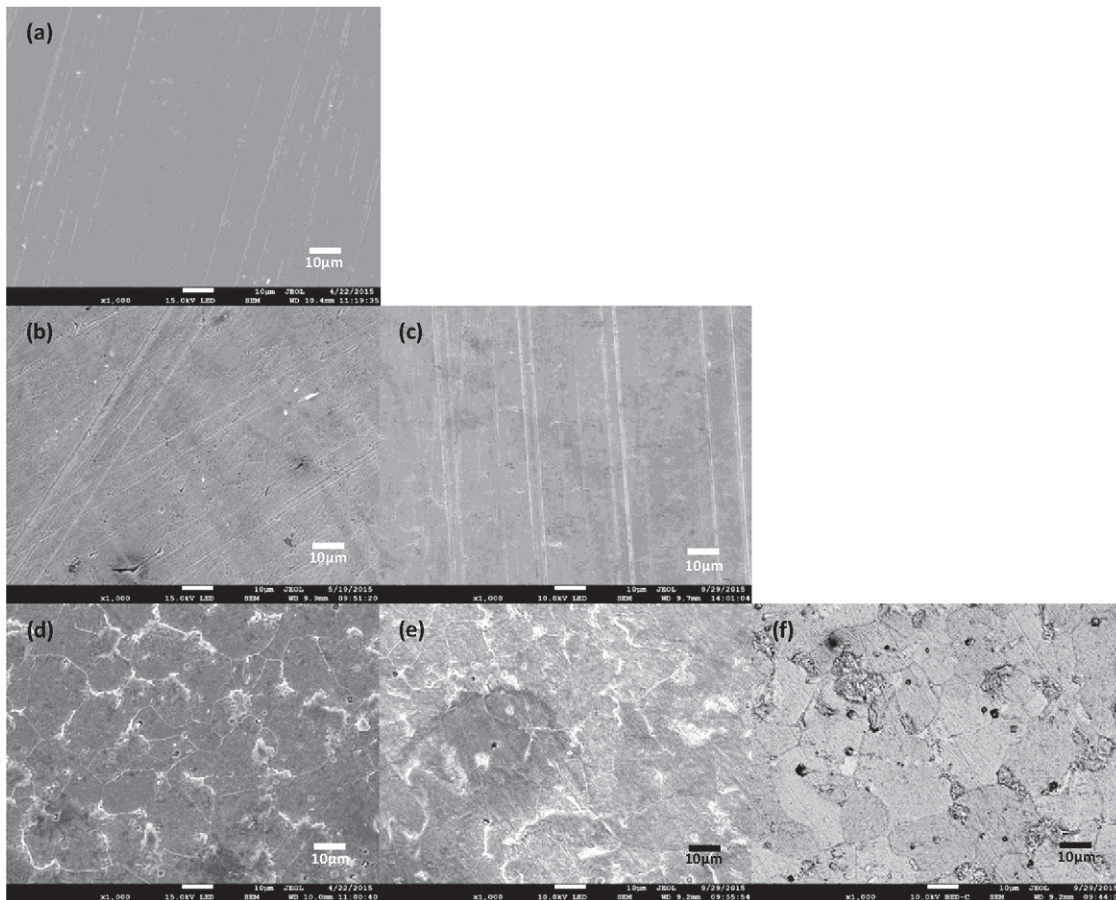


Fig. 8. SEM images of the S235JR mild steel electrode surface (a) just before immersion (24 h after grinding) (b–f) after 24 h in Tris-HCl medium with or without hydrogenase inside the dialysis bag (b) 75 μ L control solution, (c) 160 μ L control solution, (d) 75 μ L hydrogenase solution 2, (e–f) 160 μ L hydrogenase solution 3, (f) backscatter image.

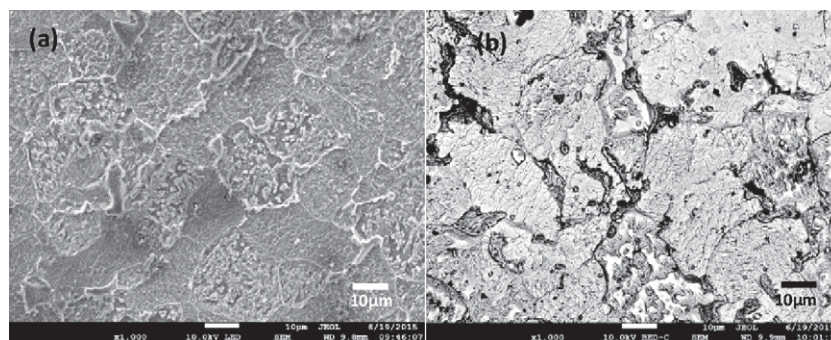


Fig. 9. SEM images of the S235JR mild steel electrode surface after a 3% nital attack (for 2 min, at ambient temperature), (a) classical image, (b) backscatter image.

Table 4
Variation in time of impedance parameters corresponding to E_{oc} measurement from Fig. 6, for S235JR mild steel electrodes with injection of 160 μL of hydrogenase solution 3 at $t=0^+$. R_s = solution resistance, R_1 and R_2 = resistances corresponding to the circle diameters at HF and MF respectively; Q_1 , α_1 and Q_2 , α_2 = characteristic parameters of CPE at HF and MF respectively; C_1 and C_2 = capacitances calculated at HF and MF respectively; δ = thickness of the oxide film.

t (h)	R_s (Ωcm^2)	High Frequency domain (HF)					Medium Frequency domain (MF)			
		R_1 (Ωcm^2)	Q_1 ($\text{F.s}\alpha^{-1}$)	α_1	C_1 ($\mu\text{F}/\text{cm}^2$)	δ (nm)	R_2 (Ωcm^2)	Q_2 ($\text{F.s}\alpha^{-1}$)	α_2	C_2 ($\mu\text{F}/\text{cm}^2$)
0	66	28	2.7×10^{-5}	0.9	4	248	1147	1.5×10^{-3}	0.7	133
5	63	29	7.9×10^{-5}	0.8	4	276	156	1.9×10^{-3}	0.7	183
24	58	24	2.4×10^{-4}	0.7	9	120	1549	1.5×10^{-3}	0.8	210

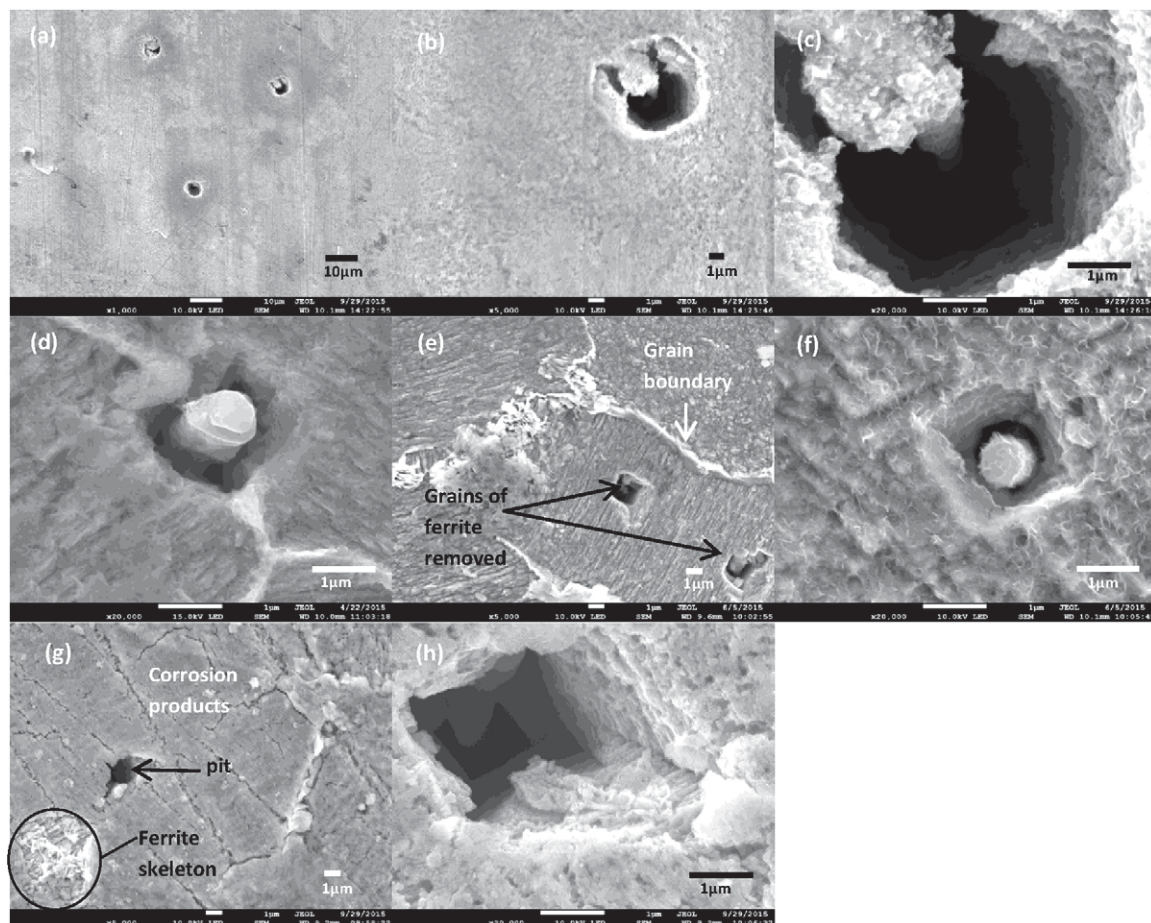


Fig. 10. SEM images of the S235JR mild steel electrode surface after 24 h in Tris-HCl medium with or without hydrogenase inside the dialysis bag. (a-c) 160 μL control solution, (d) 75 μL hydrogenase solution 2, (e and f) 75 μL hydrogenase solution 2, surface of electrodes cleaned with 50% vol. HCl and 2.5 g/L EDTA for 30s, (g and h) 160 μL hydrogenase solution 3.

current density variation was monitored over time for the injection of 75 μL hydrogenase solution 2 and its controls (Fig. 11(a)). Current density differences (Δj) were calculated in the same way as the potential ennoblement (ΔE) and their evolution with time is reported in Fig. 11(b).

The injection of control solution induced a more rapid decrease of the absolute current density, which tended to 0 mA/cm^2 . By injecting hydrogenase, the absolute current density was rapidly increased, reaching a maximum in the first hour ($\Delta j = 0.25 \text{ mA}/\text{cm}^2$). This result proved that hydrogenase catalysed the cathodic reaction to produce hydrogen from protons or water by taking electrons directly from the surface of the mild steel electrode. Thus, it is clearly demonstrated that hydrogenase is involved in a cathodic depolarisation process that accelerates corrosion of mild steel.

Moreover, after the optimum, the absolute current density decreased, tending to zero current, as in the controls. This decrease

could be possibly attributed to hydrogenase desorption and/or its deactivation, and/or changes in the active surface area of the mild steel electrode (partially because of the presence of dithionite and desthiobiotin or deactivated enzyme that could mask the surface). Some further experiments are in progress in order to understand this evolution of the current density.

3.6. Discussion

All the results showed that hydrogenase had a real impact on the corrosion of mild steel, provided that enough enzyme reached the steel surface. The new experimental setup using a dialysis bag (setup 2) permitted a better expression of this impact: confining the enzymatic solution in the close vicinity of the electrode surface allowed a larger amount of hydrogenase to reach the mild steel surface, to adsorb onto it and react with it.

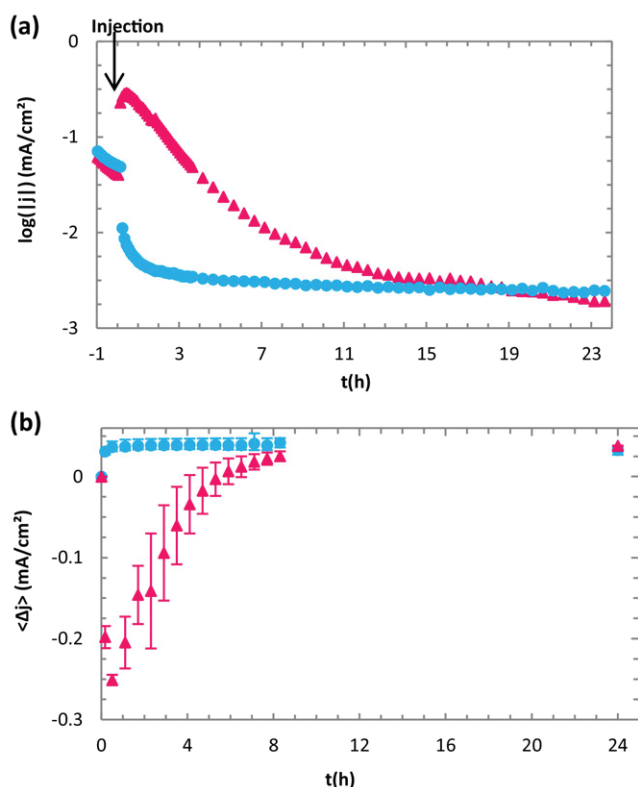


Fig. 11. Electrolysis of S235JR mild steel electrodes plotted at -100 mV vs E_{oc} in 0.1 M Tris-HCl pH7 medium inside the dialysis bag. Injection at $t=0^*$ of Δ : $75\ \mu\text{L}$ hydrogenase solution 2, \circ : $75\ \mu\text{L}$ Control solution. (a) log of cathodic current density in absolute values versus time. (b) Cathodic current density ennoblement ($\langle \Delta j \rangle = j(t) - j(t=0)$) versus time. (For interpretation of the references to colour in this figure legend, the reader is referred to the web version of this article.)

In presence of hydrogenase, there was always an increase of the open circuit potential (E_{oc}), which occurred in the first hours: a minimal concentration of enzyme in the close vicinity of the material surface was, however, required for this E_{oc} jump to be observed. With an enzyme concentration of 54.9 nM , the effect on E_{oc} was maximal (optimal E_{oc} jump). Increasing the amount of enzyme did not lead to a new increase of E_{oc} , but allowed its stabilization: an enzyme reserve is then available, new hydrogenases could adsorb on the surface, while some others could drop off.

Moreover, this potential ennoblement was always associated with an increase of the corrosion rate as shown by the measurement of the polarisation resistance (R_p) (Fig. 3) and of the charge transfer resistance obtained by impedance measurement (Figs. 4 and 6, Tables 3 and 4). Unlike the injection of control solution (for which very low $1/R_p$ values were observed), the injection of hydrogenase always led to an increase of $1/R_p$. Impedance experiments confirmed these findings: 5 h after hydrogenase injection, the charge transfer resistance had decreased markedly (divided by a factor 7), which meant that the electronic exchanges at the steel/electrolyte interface were increased.

Furthermore, after 24 h of immersion in presence of hydrogenase, the surface of mild steel was always observed to be more attacked (Figs. 8 and 10), especially at grain boundaries, and pits could reach a depth of $10\ \mu\text{m}$. Also, a greater dissolution of iron was proved to occur by ICP measurements (Table 5).

Finally, electrolysis performed at a cathodic potential confirmed that hydrogenases catalysed the cathodic reaction (reduction of protons or water) by direct electron transfer, in the very first hours of immersion (Fig. 11). A model representing the action of hydrogenase to enhance the corrosion process is proposed in Fig. 12. For

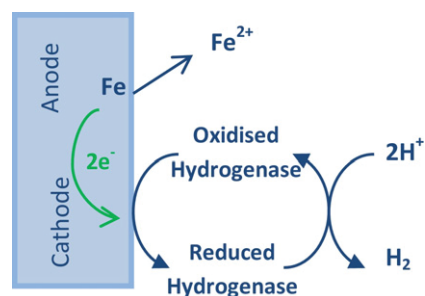


Fig. 12. Model proposed for cathodic electron depolarisation by hydrogenases (direct electron transfer), which led to a corrosion process exacerbation.

the corrosion process, hydrogenases in their oxidized state are able to take the electrons released from the metal dissolution, directly at the surface of the mild steel. Once hydrogenases are in a reduced state, they can produce hydrogen using electrons from the previous reaction. Thus, by catalysing the reduction reaction, hydrogenase promotes the cathodic depolarisation that leads to an exacerbation of mild steel corrosion (increase of the corrosion potential, rate and degradation).

Three main parameters had real importance in the expression of hydrogenase impact: the injected volume, the concentration of hydrogenase and the hydrogenase activity. Generally speaking, a minimum amount of enzyme in the close vicinity of the material surface was needed. This minimum amount had to counterbalance the inhibiting effect of the additional molecules (dithionite and desthiobiotin) present in the injected solutions. For instance, the low volume of $7.5\ \mu\text{L}$ was not sufficient to show any impact of hydrogenase on the E_{oc} evolution (Fig. 2 and Table 2) but enough for a clear influence on the evolution of the corrosion rate to be observed in a comparison with control tests (Fig. 3). Increasing the injected volume increased the quantity of enzyme and consequently led to increased corrosion. For a given injected volume, increasing the concentration (comparison between the two setups for $75\ \mu\text{L}$ and a tenfold higher concentration, Fig. 2, Fig. 3 and Table 2) clearly increased the parameters measured (E_{oc} and $1/R_p$). However, a threshold was rapidly reached: injecting $150\ \mu\text{L}$ solution 2 in setup 2 (instead of $75\ \mu\text{L}$) induced no new increase in the parameters; only a stabilization of E_{oc} and a less abrupt variation of $1/R_p$ could be observed. Actually, beyond around 55 nM , there were enough enzymes for a maximum effect to be observed and the enzyme excess enabled this maximum to be maintained. Lastly, for the same enzyme concentration, the increase of activity (16 U instead of 9 U) led to the same conclusions: a stabilization of E_{oc} and a slower decrease of corrosion rate (high R_{ct} observed 5 h after injection, Fig. 6 and Table 4).

All the experiments showed that the impact of hydrogenase was fast (optimum around one hour). In some cases, the effect was brief – most probably because of desorption of hydrogenase and/or its deactivation (change in its conformation that did not allow the transfer of electrons to the catalytic centre), and/or changes in the surface state of the mild steel electrode. But, with a concentration/activity sufficient to provide a reserve of enzyme (still active) in solution, the exacerbating effect on corrosion could be observed over several hours.

4. Conclusion

The use of a dialysis bag to concentrate [Fe-Fe]-hydrogenase from *Clostridium acetobutylicum* in the vicinity of the mild steel electrode led to conclusive tests showing the high efficiency of hydrogenase to accelerate the corrosion of S235JR mild steel. The impact was higher and/or maintained when the quantity of enzyme

increased. In fact, in presence of hydrogenases, there was always an increase of $1/R_p$ (as well as the corrosion rate) and E_{oc} whereas, with control solutions, a decrease in the parameters was always measured. Impedance experiments confirmed the strong effect of hydrogenases in increasing the corrosion of mild steel (a drastic decrease in R_{ct} by a factor 7 after 5 h). Electrolysis performed at a cathodic potential proved that hydrogenases catalysed the cathodic reaction (reduction of protons or water) by direct electron transfer, in the very first hours of immersion, proving the involvement of hydrogenase in the cathodic depolarisation process on mild steel.

Thus, the exacerbation of the corrosion process by hydrogenase is related to:

1. the volume of hydrogenase injected, which has to be sufficient to allow a visible counteraction of the inhibiting effect of additional molecules.
2. its concentration. Increasing the amount of hydrogenase in the vicinity of the electrode surface increased the response of mild steel: more hydrogenase was adsorbed on the electrode surface until a saturation plateau of E_{oc} was reached
3. its enzymatic activity. Higher activity implied the same jump and then stabilization of E_{oc} and a less abrupt decrease of $1/R_p$ (after reaching the maximum).

The impact of hydrogenase to induce cathodic depolarisation is a transient phenomenon, which could explain why corrosion in presence of hydrogenase is still a controversial subject. Work is in progress to understand this transient effect and the mechanisms involved.

Acknowledgements

The authors would like to thank Charles Gauquelin and Isabelle Meynial-Salles for providing [Fe-Fe]-hydrogenases from *C. acetobutylicum* and activity tests. We also thank Marie-Line De Solan Bethmale for assistance with SEM imaging and ICP, and Susan Becker, freelance translator, for her help with the English. This work was financially supported by the French "Ministère de l'Enseignement Supérieur".

Appendix A. Supplementary data

Supplementary data associated with this article can be found, in the online version, at <http://dx.doi.org/10.1016/j.corsci.2016.05.005>.

References

- [1] M. Madigan, Brock Biology of Microorganisms, Pearson Prentice Hall, Upper Saddle River NJ, 2006.
- [2] M. Calusinska, T. Happe, B. Joris, A. Wilmette, The surprising diversity of clostridial hydrogenases: a comparative genomic perspective, *Microbiology* 156 (2010) 1575–1588, <http://dx.doi.org/10.1099/mic.0.032771-0>.
- [3] J.S. Deutzmann, M. Sahin, A.M. Spormann, Extracellular enzymes facilitate electron uptake in biocorrosion and bioelectrosynthesis, *MBio* 6 (2015) 00496–515, <http://dx.doi.org/10.1128/mbio.00496-15>.
- [4] L.-F. Wu, M.A. Mandrand, Microbial hydrogenases: primary structure, classification, signatures and phylogeny, *FEMS Microbiol. Lett.* 104 (1993) 243–270, <http://dx.doi.org/10.1111/j.1574-6968.1993.tb05870.x>.
- [5] M. Mehanna, R. Basseguy, M.-L. Delia, L. Girbal, M. Demuez, A. Bergel, New hypotheses for hydrogenase implication in the corrosion of mild steel, *Electrochim. Acta* 54 (2008) 140–147, <http://dx.doi.org/10.1016/j.electacta.2008.02.101>.
- [6] S. Da Silva, R. Basséguy, A. Bergel, Electron transfer between hydrogenase and 316L stainless steel: identification of a hydrogenase-catalyzed cathodic reaction in anaerobic mic, *J. Electroanal. Chem.* 561 (2004) 93–102, <http://dx.doi.org/10.1016/j.jelechem.2003.07.005>.
- [7] F. Van Ommen Kloeke, R.D. Bryant, E.J. Laishley, Localization of cytochromes in the outer membrane of *Desulfovibrio vulgaris* (Hildenborough) and their role in anaerobic biocorrosion, *Anaerobe* 1 (1995) 351–358, <http://dx.doi.org/10.1006/anae.1995.1038>.
- [8] A.V. Ramesh Kumar, R. Singh, R.K. Nigam, Mössbauer spectroscopy of corrosion products of mild steel due to microbiologically influenced corrosion, *J. Radioanal. Nucl. Chem.* 242 (1999) 131–137, <http://dx.doi.org/10.1007/BF02345906>.
- [9] J.F.D. Stott, What progress in the understanding of microbially induced corrosion has been made in the last 25 years? A personal viewpoint, *Corros. Sci.* 35 (1993) 667–673, [http://dx.doi.org/10.1016/0010-938X\(93\)90202-R](http://dx.doi.org/10.1016/0010-938X(93)90202-R).
- [10] H. Venzlaff, D. Enning, J. Srinivasan, K.J.J. Mayrhofer, A.W. Hassel, F. Widdel, et al., Accelerated cathodic reaction in microbial corrosion of iron due to direct electron uptake by sulfate-reducing bacteria, *Corros. Sci.* 66 (2013) 88–96, <http://dx.doi.org/10.1016/j.corsci.2012.09.006>.
- [11] C. Chatelus, P. Carrier, P. Saignes, M.F. Libert, Y. Berlier, P.A. Lespinat, et al., Hydrogenase activity in aged, nonviable *Desulfovibrio vulgaris* cultures and its significance in anaerobic biocorrosion, *Appl. Environ. Microbiol.* 53 (1987) 1708–1710 (accessed 26.10.15) <http://www.pubmedcentral.nih.gov/articlerender.fcgi?artid=203938&tool=pmcentrez&rendertype=abstract>.
- [12] M.D. Yates, M. Siegart, B.E. Logan, Hydrogen evolution catalyzed by viable and non-viable cells on biocathodes, *Int. J. Hydrogen Energy* 39 (2014) 16841–16851, <http://dx.doi.org/10.1016/j.ijhydene.2014.08.015>.
- [13] D.J. Evans, C.J. Pickett, Chemistry and the hydrogenases, *Chem. Soc. Rev.* 32 (2003) 268–275, <http://dx.doi.org/10.1039/b201317g>.
- [14] Y. Nicolet, C. Cavazza, J.C. Fontecilla-Camps, Fe-only hydrogenases: structure, function and evolution, *J. Inorg. Biochem.* 91 (2002) 1–8, [http://dx.doi.org/10.1016/S0162-0134\(02\)00392-6](http://dx.doi.org/10.1016/S0162-0134(02)00392-6).
- [15] P.M. Vignais, A. Colbeau, Molecular biology of microbial hydrogenases, *Curr. Issues Mol. Biol.* 6 (2004) 159–188 (accessed 01.07.15) <http://www.ncbi.nlm.nih.gov/pubmed/15119826>.
- [16] F.A. Armstrong, Hydrogenases: active site puzzles and progress, *Curr. Opin. Chem. Biol.* 8 (2004) 133–140, <http://dx.doi.org/10.1016/j.cbpa.2004.02.004>.
- [17] A. Volbeda, J.C. Fontecilla-Camps, Structure–function relationships of nickel–iron sites in hydrogenase and a comparison with the active sites of other nickel–iron enzymes, *Coord. Chem. Rev.* 249 (2005) 1609–1619, <http://dx.doi.org/10.1016/j.ccr.2004.12.009>.
- [18] R.D. Bryant, W. Jansen, J. Boivin, E.J. Laishley, J.W. Costerton, Effect of hydrogenase and mixed sulfate-reducing bacterial populations on the corrosion of steel, *Appl. Environ. Microbiol.* 57 (1991) 2804–2809 (accessed 26.04.13) <http://aem.asm.org/content/57/10/2804>.
- [19] L. De Silva Muñoz, A. Bergel, R. Basséguy, Role of the reversible electrochemical deprotonation of phosphate species in anaerobic biocorrosion of steels, *Corros. Sci.* 49 (2007) 3988–4004, <http://dx.doi.org/10.1016/j.corsci.2007.04.003>.
- [20] S. Da Silva, R. Basseguy, A. Bergel, A new definition of cathodic depolarization in anaerobic MIC, *Corrosion* 2002 (2002) (accessed 16.03.16) <https://www.onepetro.org/conference-paper/NACE-02462>.
- [21] F.A. Armstrong, J. Hirst, Reversibility and efficiency in electrocatalytic energy conversion and lessons from enzymes, *Proc. Natl. Acad. Sci. U. S. A.* 108 (2011) 14049–14054, <http://dx.doi.org/10.1073/pnas.1103697108>.
- [22] T. Reda, C.M. Plugge, N.J. Abram, J. Hirst, Reversible interconversion of carbon dioxide and formate by an electroactive enzyme, *Proc. Natl. Acad. Sci. U. S. A.* 105 (2008) 10654–10658, <http://dx.doi.org/10.1073/pnas.0801290105>.
- [23] M. Mehanna, R. Basseguy, M.-L. Delia, A. Bergel, Role of direct microbial electron transfer in corrosion of steels, *Electrochem. Commun.* 11 (2009) 568–571, <http://dx.doi.org/10.1016/j.elecom.2008.12.019>.
- [24] M. Libert, M.K. Schütz, L. Esnault, D. Féron, O. Bildstein, Impact of microbial activity on the radioactive waste disposal: long term prediction of biocorrosion processes, *Bioelectrochemistry* 97 (2014) 162–168, <http://dx.doi.org/10.1016/j.bioelechem.2013.10.001>.
- [25] M. Rosenbaum, F. Aulenta, M. Villano, L.T. Angenent, Cathodes as electron donors for microbial metabolism: which extracellular electron transfer mechanisms are involved? *Bioresour. Technol.* 102 (2011) 324–333, <http://dx.doi.org/10.1016/j.biortech.2010.07.008>.
- [26] E. Lojou, Hydrogenases as catalysts for fuel cells: strategies for efficient immobilization at electrode interfaces, *Electrochim. Acta* 56 (2011) 10385–10397, <http://dx.doi.org/10.1016/j.electacta.2011.03.002>.
- [27] M. Hamburger, M. Gervaldo, D. Svedruzic, P.W. King, D. Gust, M. Ghirardi, et al., [FeFe]-hydrogenase-catalyzed H₂ production in a photoelectrochemical biofuel cell, *J. Am. Chem. Soc.* 130 (2008) 2015–2022, <http://dx.doi.org/10.1021/ja077691k>.
- [28] M.J. Lukey, A. Parkin, M.M. Roessler, B.J. Murphy, J. Harmer, T. Palmer, et al., How *Escherichia coli* is equipped to oxidize hydrogen under different redox conditions, *J. Biol. Chem.* 285 (2010) 3928–3938, <http://dx.doi.org/10.1074/jbc.M109.067751>.
- [29] A. de Poulpique, A. Ciaccavava, R. Gadiou, S. Gounel, M.T. Giudici-Orticoni, N. Mano, et al., Design of a H₂/O₂ biofuel cell based on thermostable enzymes, *Electrochem. Commun.* 42 (2014) 72–74, <http://dx.doi.org/10.1016/j.elecom.2014.02.012>.
- [30] C. Baffert, K. Sybirna, P. Ezanno, T. Lautier, V. Hajji, I. Meynial-Salles, et al., Covalent attachment of FeFe hydrogenases to carbon electrodes for direct electron transfer, *Anal. Chem.* 84 (2012) 7999–8005, <http://dx.doi.org/10.1021/ac301812s>.
- [31] B. Soni, P. Soucaille, G. Goma, Continuous acetone-butanol fermentation – influence of vitamins on the metabolic-activity of *Clostridium acetobutylicum*, *Appl. Microbiol. Biotechnol.* 27 (1987) 1–5 (accessed 13.05.13) http://apps.wobofknowledge.com/full_record.do?product=UA&search_mode=GeneralSearch&qid=20&SID=R2G95ica8jdACgna8Ab&page=1&doc=8&cacheurlFromRightClick=no.

- [32] J.C. Fontecilla-Camps, A. Volbeda, C. Cavazza, Y. Nicolet, Structure/function relationships of [NiFe]- and [FeFe]-hydrogenases, *Chem. Rev.* 107 (2007) 4273–4303, <http://dx.doi.org/10.1021/cr050195z>.
- [33] L. Girbal, G. von Abendorth, M. Winkler, P.M.C. Benton, I. Meynial-Salles, C. Croux, et al., Homologous and heterologous overexpression in clostridium acetobutylicum and characterization of purified clostridial and algal Fe-Only hydrogenases with high specific activities, *Appl. Environ. Microbiol.* 71 (2005) 2777–2781, <http://dx.doi.org/10.1128/AEM.71.5.2777-2781.2005>.
- [34] I. Rouvre, C. Gauquelin, I. Meynial-Salles, R. Basseguy, Impact of the chemicals, essential for the purification process of strict Fe-hydrogenase, on the corrosion of mild steel, *Bioelectrochemistry* 109 (2015) 9–23, <http://dx.doi.org/10.1016/j.bioelechem.2015.12.006>.
- [35] T. Lautier, P. Ezanno, C. Baffert, V. Fourmond, L. Cournac, J.C. Fontecilla-Camps, et al., The quest for a functional substrate access tunnel in FeFe hydrogenase, *Faraday Discuss.* 148 (2011) 385–407 <http://pubs.rsc.org/en/content/articlehtml/2010/fd/c004099c>.
- [36] G. von Abendorth, S. Stripp, A. Silakov, C. Croux, P. Soucaille, L. Girbal, et al., Optimized over-expression of [FeFe] hydrogenases with high specific activity in *Clostridium acetobutylicum*, *Int. J. Hydrogen Energy* 33 (2008) 6076–6081, <http://dx.doi.org/10.1016/j.ijhydene.2008.07.122>.
- [37] M. Adams, L. Mortenson, The physical and catalytic properties of hydrogenase II of *Clostridium pasteurianum*. A comparison with hydrogenase I, *J. Biol. Chem.* 259 (1984) 7045–7055 (accessed 07.02.15) <http://www.jbc.org/content/259/11/7045.abstract?sid=5187eda4-5c5d-4e62-a430-e35fe77bc7da>.
- [38] C. Wagner, W. Traud, Über die deutung von korrosionsvorgängen durch Überlagerung von elektrochemischen teilvorgängen und über die potentialbildung an mischelektroden, *Zeitschrift Für Elektrochemie Und Angew. Phys. Chem.* 44 (1938) 391–402, <http://dx.doi.org/10.1002/bbpc.193804440702>.
- [39] M. Stern, A.L. Geary, Electrochemical polarization, *J. Electrochem. Soc.* 104 (1957) 56, <http://dx.doi.org/10.1149/1.2428496>.
- [40] V.M.-W. Huang, V. Vivier, I. Frateur, M.E. Orazem, B. Tribollet, The global and local impedance response of a blocking disk electrode with local constant-Phase-Element behavior, *J. Electrochem. Soc.* 154 (2007) C89, <http://dx.doi.org/10.1149/1.2398889>.
- [41] B. Hirschorn, M.E. Orazem, B. Tribollet, V. Vivier, I. Frateur, M. Musiani, Constant-Phase-Element behavior caused by resistivity distributions in films, *J. Electrochem. Soc.* 157 (2010) C452, <http://dx.doi.org/10.1149/1.3499564>.
- [42] B. Hirschorn, M.E. Orazem, B. Tribollet, V. Vivier, I. Frateur, M. Musiani, Constant-Phase-Element behavior caused by resistivity distributions in films, *J. Electrochem. Soc.* 157 (2010) C458, <http://dx.doi.org/10.1149/1.3499565>.
- [43] M.E. Orazem, I. Frateur, B. Tribollet, V. Vivier, S. Marcelin, N. Pebere, et al., Dielectric properties of materials showing constant-Phase-Element (CPE) impedance response, *J. Electrochem. Soc.* 160 (2013) C215–C225, <http://dx.doi.org/10.1149/2.033306jes>.
- [44] W.M. Haynes, *CRC Handbook of Chemistry and Physics*, 95th edition, CRC Press Inc, Taylor and Francis group, Boca Raton, London, New York, 2014 (accessed 23.10.15) <https://books.google.com/books?hl=fr&lr=&id=bNDMBQAAQBAJ&pgis=1>.
- [45] M.E. Orazem, B. Tribollet, *Electrochemical Impedance Spectroscopy*, John Wiley & Sons, Inc, Hoboken, NJ, USA, 2008.
- [46] M.E. Orazem, N. Peibeře, B. Tribollet, Enhanced graphical representation of electrochemical impedance data, *J. Electrochem. Soc.* 153 (2006) B129, <http://dx.doi.org/10.1149/1.2168377>.
- [47] C.H. Hsu, F. Mansfeld, Technical note concerning the conversion of the constant phase element parameter Y0 into a capacitance, *Corrosion* 57 (2001) (accessed 01.10.15) <https://www.onepetro.org/journal-paper/NACE-01090747>.
- [48] G.J. Brug, A.L.G. van den Eeden, M. Sluyters-Rehbach, J.H. Sluyters, The analysis of electrode impedances complicated by the presence of a constant phase element, *J. Electroanal. Chem. Interfacial Electrochem.* 176 (1984) 275–295, [http://dx.doi.org/10.1016/S0022-0728\(84\)80324-1](http://dx.doi.org/10.1016/S0022-0728(84)80324-1).
- [49] R. Avci, B.H. Davis, M.L. Wolfenden, I.B. Beech, K. Lucas, D. Paul, Mechanism of MnS-mediated pit initiation and propagation in carbon steel in an anaerobic sulfidogenic media, *Corros. Sci.* 76 (2013) 267–274, <http://dx.doi.org/10.1016/j.corsci.2013.06.049>.